Controlled Phase Separation of Polyfluorene Blends via Inkjet Printing

Yajun Xia and Richard H. Friend*

Cavendish Laboratory, Madingley Road, Cambridge CB3 0HE, UK

Received February 17, 2005; Revised Manuscript Received May 10, 2005

ABSTRACT: We report the use of inkjet printing (IJP) to produce thin polymer films with controlled phase separation of binary polymer blends. Photovoltaic devices comprising a blend of poly(9,9′-dioctyfluorene-*co*-bis-*N*,*N*′-(4-butylphenyl)-bis-*N*,*N*′-phenyl-1,4-phenylenediamine) (PFB) with poly(9,9′-dioctylfluorene-*co*-benzothiadiazole) (F8BT) and light-emitting diodes (LEDs) constituting a blend of F8BT with poly(9,9-dioctylfluorene-*co*-*N*-(4-butylphenyl)diphenylamine) (TFB) were fabricated. The phase separation in these polymer blends was analyzed using atomic force microscopy and photoluminescent optical microscopy. The lateral phase separation in both blend films spin-coated from *p*-xylene solution is typically a few microns; however, by inkjet printing a solution of an identical composition, the feature size can be reduced to ∼300 nm when combined with an elevated substrate temperature during the printing process. This results from the rapid solvent evaporation of the inkjet-printed droplets. LEDs made by IJP show well-behaved *I*−*V*−*L* characteristics, with lower current density and higher luminescent efficiency than spin-coated devices at high voltages. The finer-scale phase separation from IJP also leads to a factor of 2 improvement in the external quantum efficiencies of photovoltaic diodes.

I. Introduction

Conjugated polymers have semiconducting properties due to their delocalizing π-electrons along polymer backbones. Polymer LEDs (PLEDs) and polymer photovoltaic devices have attracted great interest since the first report of electroluminescence (EL) in conjugated polymers.[1−6] These devices comprise a spin-coated thin polymer layer sandwiched between two electrode layers. To improve charge injection/collection and charge transport, combinations of hole and electron-transporting polymers are used, often as blends codeposited from common solution, and can give efficient LEDs and photovoltaic devices.[4−8] Blends of poly(9,9-dioctylfluorene-*co*-*N*-(4-butylphenyl)diphenylamine) (TFB) with poly(9,9′-dioctylfluorene-*co*-benzothiadiazole) (F8BT) give good LEDs,[9,10] and of poly(9,9′-dioctyfluorene-*co*-bis-*N*,*N*′-(4-butylphenyl)-bis-*N*,*N*′-phenyl-1,4-phenylenediamine) (PFB) with F8BT, give good photovoltaic devices.[6,11−13] In these blend systems, there is always some degree of demixing of the two polymers during the loss of solvent, and a wide range of morphologies can be produced, ranging from micron-scale features for slow solvent evaporation to nanometer scale for rapid drying. This morphology plays an important role in device operations. Many efforts have been implemented to control the phase separation of polymer blends, including hot-spinning,[8] using low boiling point solvents,[12] and the use of polymers with lower molecular weight.[11] Here we demonstrate the formation of a controlled phase separation via inkjet printing. Inkjet printing (IJP) has been put forward as a technique to realize selective deposition of materials for electronic devices, which allows a small amount of materials to be deposited at a required position with a high degree of accuracy.[14,15] In

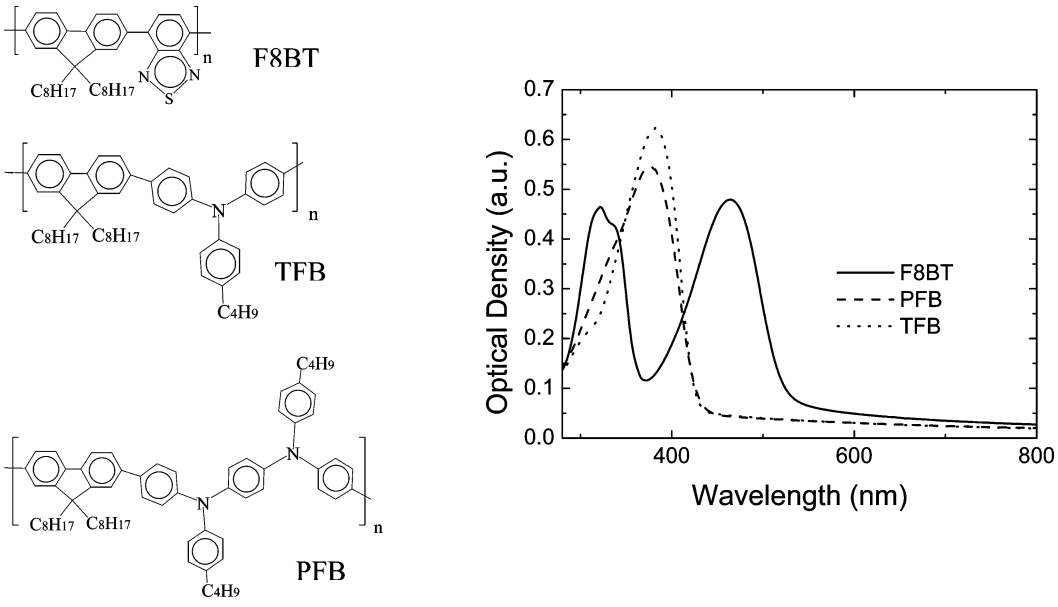

Figure 1. Chemical structures of F8BT, TFB, and PFB, together with absorption spectra (measured as −lg(transmission)) of thin films made from them.

10.1021/ma0503413 CCC: $30.25
Published on Web 06/23/2005

this report we show how IJP is used to print continuous films of semiconducting polymer blends and compare them with those prepared by spin-coating in terms of morphology, drying time, LED characteristics, and photovoltaic device performances.

II. Experimental Section

A. Sample Preparation. The polymers studied in this work were two different type II heterojunction systems of polyfluorene derivatives: a blend of hole acceptor PFB with electron acceptor F8BT and a blend of F8BT with hole acceptor TFB. The composition of TFB:F8BT and PFB:F8BT used here was both 50:50 by mass. Their chemical structures are shown in Figure 1 together with their optical absorption spectra. To make a device, glass substrates sputtered with an indium−tin oxide (ITO) layer were cleaned in an ultrasonic bath with acetone and 2-propanol in turn, each for 10 min. The substrates were then dried with nitrogen, followed by exposure to oxygen plasma for 10 min at forward power of 250 W, resulting in a hydrophilic surface that wets the water-based solution well. A layer of poly(3,4-ethylene dioxythiopene) (PEDOT), from H.C. Starck, doped with poly(4-styrenesulfonate) (PSS), was spin-coated from an aqueous solution, with a thickness of roughly 60 nm after drying. The substrate was then baked on a hot plate in nitrogen at 150 °C for 30 min. A layer of semiconducting polymer was deposited by either spin-coating or inkjet printing a polymer solution (prepared in *p*-xylene) on the PEDOT:PSS layer. Cathodes (Ca, Al, or Cu) were then deposited by thermal evaporation through a shadow mask, at a base pressure lower than 3×10^{-6} mbar.

B. Inkjet Printing. A custom-built inkjet printer incorporating a piezoelectric inkjet head manufactured by Seiko Epson and a motorized translation stage were used to pattern polymer films. For compatibility with organic solvents, aluminum parts replaced some plastic parts of the head. The device substrate was placed ~2 mm below the inkjet head. To elevate the temperature of the substrate, an ITO-coated glass slide was inserted under the device substrate during printing and used as a resistive heater by allowing electrical current to flow through the ITO surface. The substrate temperature was tuned over a range of 20−40 °C to control the phase separation of inkjet printed blended polymer films. The printer was operated at about 100 drops/s; the volume of each printed droplet was estimated to be on the order of 50 pL. A continuous film of polymer was printed line-by-line with neighboring strips adjacent to each other, so as to prevent subsequent short circuits between electrodes after metal evaporation.

C. Photoluminescence Measurements. To characterize photoluminescence (PL), polymer films were deposited onto spectrosil B substrates. The precleaning of these substrates followed the same procedure described above for ITO-coated substrates. The PL spectrum was collected by an Oriel spectrometer (InstaSpec IV CCD−matrix system), under the excitation of 457 nm from an Ar^+ laser. The quantum yield of photoluminescence was determined using an integrating sphere.[16]

D. Morphology. The PL and electroluminescence (EL) microscopic structures of blend films were observed through a fluorescent microscope (Olympus BX60), under excitations of wide-band UV or blue illumination, or of an operating voltage. PLEDs were encapsulated prior to microscopic observation in air. Atomic force microscopy (AFM, NanoScope IIIa Dimension 3100, Digital Instrument Inc.) was used to study surfaces of these blend films.

III. Results and Discussion

A. Thickness Profile of IJP Films. Figure 2a shows a thickness profile across one single IJP line of F8BT, showing the thickness variation perpendicular to the printing direction. The central portion of the film is about 70 nm, much thinner than at the edge region of more than 200 nm. Because of the pinning of the contact

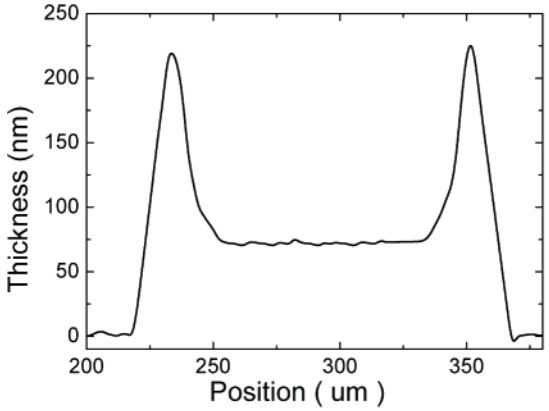

(a)

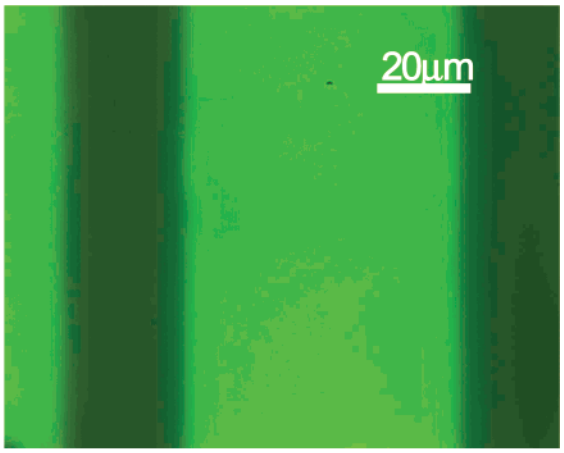

(b)

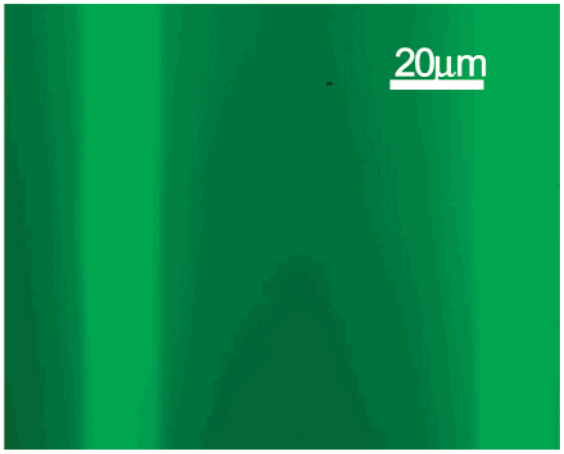

(c)

Figure 2. Thickness profile across a single IJP line of F8BT measured by Dektak II (a); EL (b) and PL (c) images of an IJP film made from the TFB:F8BT blend. PL image is taken with excitation at 457 nm so that only F8BT is excited. The bright lines in (c) indicate the thicker edges of the IJP strips and correspond to the dark edges in (b).

line between a printed droplet and the substrate, a capillary flow takes place from the interior of the droplet to the edge area during the evaporation of solvents.[17−19] This "coffee-stain" effect[18] reproducibly gives this nonuniform film thickness. Such a distribution in the thickness of a semiconductor film has a dramatic influence on the operation of electroluminescent devices

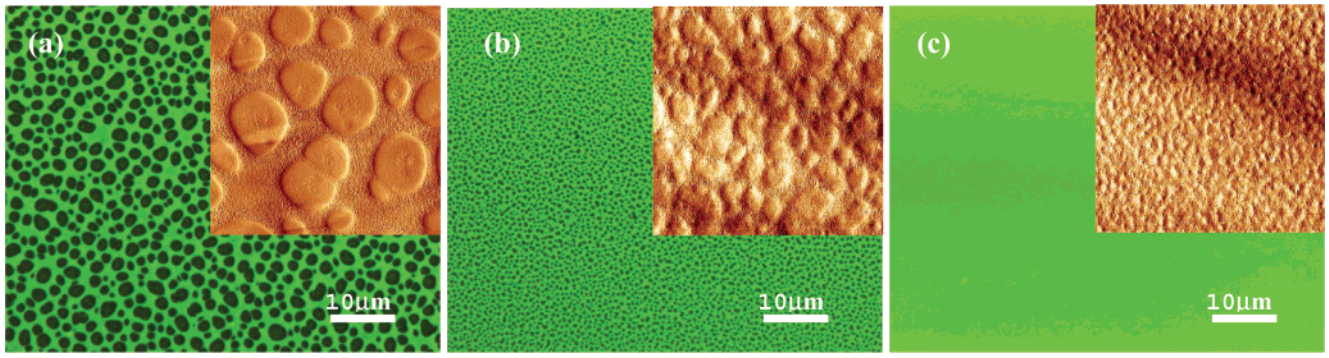

Figure 3. Fluorescent microscopic pictures of TFB:F8BT blend films produced by spin-coating (a), IJP at room temperature (RT) (b), and IJP at 40 °C (c). The insets are AFM pictures (10 × 10 μm) taken on them. Blend films were deposited onto ITO-coated substrates.

since the edge area is simply too thick to work. However, the edge region occupies only 20−30% of the total area of one printed strip, leaving the remaining area relatively flat, which means the effectively functional area is 70−80% of the total IJP film. The EL image of an IJP LED in Figure 2b shows the contrast in electroluminescent intensity between these two regions. Figure 2c shows a PL image of the same area taken under blue radiation. It can be seen that the bright area in PL image corresponds to the dark edges in the EL picture.

B. Morphology. Spin-coating a film of TFB:F8BT blend from the common solution using *p*-xylene as solvent usually yields a lateral phase separation of the order of a few microns.[9] This can be easily observed by selective absorption using fluorescent microscopy, whereby under blue excitation the regions that emit a yellowish-green light correspond to F8BT phase, and the areas remaining dark correspond to the TFB phase (Figure 3a). Islands of TFB up to a few micrometers in size are surrounded by F8BT. As also observed by AFM, the TFB islands are actually suppressed to the ITO substrate surface, with F8BT region raised by averagely ∼20 nm for a ∼60 nm spin-coated film. Roughness analysis on AFM picture reveals that the root-mean-square roughness (R_{rms}) over 10 × 10 μm is ∼8.4 nm. It has also been found from Raman spectroscopy that the TFB-rich domains have a small amount of F8BT (∼20−25%), and F8BT-rich domains contain about 30−35% TFB and are associated with further, submicron scale phase separation.[9]

When the blend film is formed by IJP, the feature size of lateral phase separation is reduced to around 1 μm (Figure 3b). Although F8BT-rich regions are still thicker, the film smoothness is greatly improved, with the rms surface height fluctuation reduced to ∼4.3 nm. By increasing the temperature of the underlying substrates slightly during printing (up to about 40 °C), the lateral phase separation is further reduced to about 300 nm, which is beyond the resolution of the optical measurement (Figure 3c). The surface becomes very smooth, with height fluctuation being reduced to ∼1.7 nm. Similar results are obtained from PFB:F8BT blend. It should be noted at this stage that the phase separation is of the size of a few hundred nanometers to a few microns, which is considerably larger than the molecular size.

The suppressed phase separation of IJP films arises from its more rapid drying process in comparison with spin-coating. Because of the small volume of each IJP drop (about 50 pL), the solvent evaporates much more quickly than spin-coating. This gives less time to allow the two polymers to demix from each other, which consequently produces a finer-scale phase separation. From visual observation of deposited drops from *p*-xylene solution, we estimate the drying time of a spin-coated film at room temperature is about 10−20 s; however, for IJP lines it is about 4 s at room temperature and is reduced to below 1 s when the substrate is heated to 40 °C. It is worth mentioning that the IJP process allows convenient control of the temperature of a substrate, in contrast to spin-coating.

C. LED Characteristics. The *I*−*V*−*L* characteristics of inkjet printed and spin-coated LEDs are shown in Figure 4. Devices prepared by inkjet printing compare favorably with those by spin-coating, with a similar turn-on voltage and low leakage current (<10^{-3} mA/cm^2). The turn-on voltage is about 1.8 V, with a current density of ∼0.14 V/decade after turn-on. However, for devices inkjet printed at ∼40 °C with the same active layer thickness as that of spin-coated devices, a lower current density is measured at high operating voltages (Figure 4a).

The higher current density of spin-coated devices is very likely due to higher hole current flowing across the thinner TFB phases in spin-coated films. To verify this, we compare blend devices of the same thickness made by spin-coating at room temperature and IJP at 40 °C, with PEDOT:PSS as anode and Cu as cathode. A hole current is generated because the barrier for electron injection is high, as shown in the inset of Figure 4b.[9,20] We found that the current density of spin-coated device is about 2−3 times of that of IJP device (Figure 4b). At higher voltages the current is space charge limited. The space charge limited (SCL) current of single carriers is given by[21]

$$J = \frac{9}{8}\epsilon\epsilon_0\mu V^2/d^3$$

where $\epsilon\epsilon_0$ is the permittivity of polymer, μ is the carrier mobility, and d is the film thickness. Assuming the TFB phase of IJP and spin-coated blend films have the same permittivity ($\epsilon = 3$) and hole mobility, and both of them occupy nearly 50% of the total film area, the J−V curves are well fitted by the SCL model at high voltages, using hole mobility $\mu = \sim 7 \times 10^{-7}$ cm^2/(V s). The SCL model predicts the TFB regime of spin-coated blend films is of average thickness ∼42 nm, roughly 30% thinner than that of blend film prepared by IJP at 40 °C, consistent with the experimental observations from the AFM analysis in Figure 3. If we suppose the TFB regime has a similar hole mobility as the electron mobility of F8BT

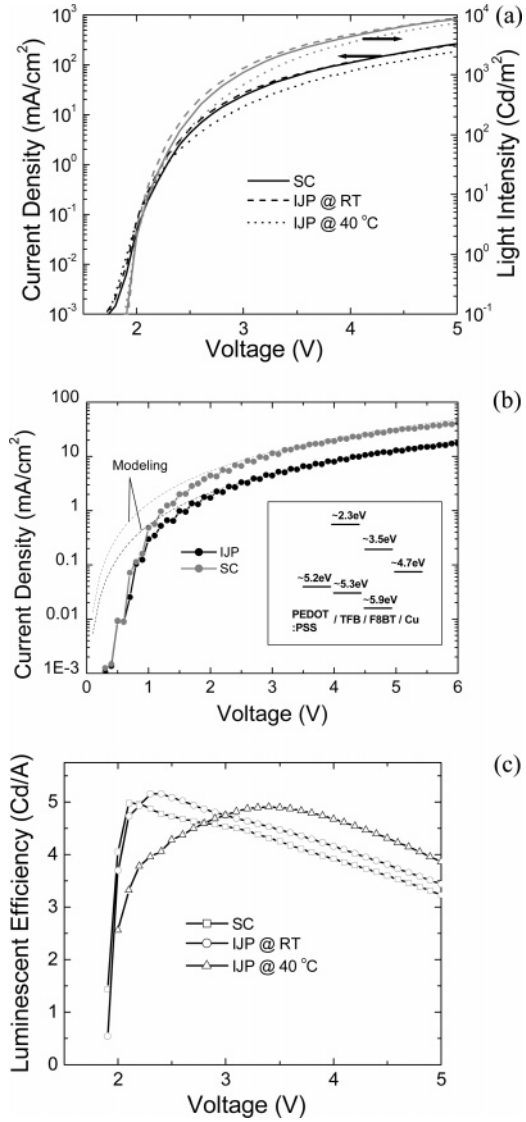

Figure 4. (a) $I-V-L$ characteristics of TFB:F8BT blend LEDs produced by spin-coated (solid line), IJP at room temperature (dashed line), and IJP at 40 °C (dotted line) (black lines: current density; gray lines: light intensity; the current density of IJP at room temperature devices slightly overlaps with that of spin-coated devices); (b) the $I-V$ comparison between blend devices prepared by spin-coating (gray circles) and IJP at 40 °C (black circles), using PEDOT:PSS as anode and Cu as cathode; the inset is energy diagrams of relevant polymers and electrodes; (c) the luminescent efficiency of devices in (a), produced by spin-coating (squares), IJP at room temperature (circles), and IJP at 40 °C (triangles). The LED structure is ITO/PEDOT:PSS/polymer/Ca/Al (60 nm PEDOT:PSS, 60 nm polymer film for spin-coating and IJP at 40 °C, 50 nm polymer film for IJP at room temperature, 100 nm Ca, and 200 nm Al).

regime, and they occupy nearly the same area, then for blend LEDs the current in the spin-coated device should double that in the printed device. In reality, this simplified model is complicated by charge recombination and neutralization within the film. The actual spin-coated device current is about 50−70% higher than that in IJP device.

We observe that the IJP and spin-coated LED devices have a similar maximum external efficiency, but a very different dependence on voltage. For a blend device of about 60 nm film, the efficiency of spin-coated device goes up sharply after its turn-on and reaches its maximum at about 2.1 V and then drops down straight afterward; for devices inkjet printed at room temperature, the efficiency curve has a similar shape, but the voltage at maximum efficiency is shifted to ∼2.4 V; however, for devices inkjet printed at 40 °C, the efficiency rises slowly after turn-on, surpasses that of the spin-coated device at ∼2.7 V, and reaches its maximum at ∼3.5 V.

It is of great interest to see the hot-IJP blend devices have higher efficiency at high voltages. It is not completely understood yet why the luminescent efficiency of IJP and spin-coated LEDs have such a different dependence on voltage. It has been proposed that in the blend system of TFB:F8BT the electrons and holes undergo a free-barrier capture process at the heterojunction between F8BT and TFB, which is a very efficient process due to the lower necessary electric field across the heterojunction.[6] In this case, more interfaces in IJP blends simply mean more chances of electron−hole capture. Another reason may be due to the lower hole "leakage" current of the IJP device as discussed above, which flows through the thinner TFB. However, this does not explain why the spin-coated device has higher efficiency at low voltages. One possible factor is that IJP and spin-coated devices have different vertical phase separation structures. It has been reported that the spin-coated TFB blend has a thin TFB wetting layer close to anode.[9] This wetting layer acts as a hole accepting/transporting and electron-blocking layer, which favors the operation of devices at low voltages. However, so far it is not clear yet whether a similar wetting layer exists in IJP films.

We note that the device efficiency in our experiments is not as high as reported by industrial groups,[6] and this is due to the lower level of process control available to us. However, this still allows us to compare the results of IJP and spin-coating under different processing conditions.

D. Photovoltaic Characteristics. The fine-scale phase separation arising from IJP produces very efficient photovoltaic devices, as shown in Figure 5. For the PFB:F8BT blend, the external quantum efficiency (EQE) (the number of electrons collected in the external circuit per incident photon) of IJP devices is higher than spin-coated devices over all the spectrum for a 60 nm thick film (Figure 5a). In particular, the devices prepared by IJP at 40 °C exhibit an EQE more than twice that of spin-coated devices.

The quantum efficiency of blend devices depends strongly on their morphology.[8,11] In the blend of PFB:F8BT, it has been suggested that it is charge transport, as opposed to charge dissociation, that limits the quantum efficiency of blend devices.[11] Table 1 shows the PL efficiency of spin-coated and IJP blends of PFB:F8BT under the excitation of 457 nm. It is seen when the phase separation of PFB:F8BT blends goes from the size of few micrometers down to about 300 nm produced by IJP at 40 °C (similar to TFB:F8BT blend), the PL efficiency changes very little, which implies there is almost no change in quenching due to charge dissociation. This indicates that phase separation at molecular scale is not changed significantly. We consider therefore that the higher EQE in IJP devices is due to improved charge transport. The EQE is further improved when the cathode is changed from Al to Ca. The increased EQE of Ca devices is most likely due to the enhanced internal electrical field caused by the work function mismatch between anode and cathode, which leads to

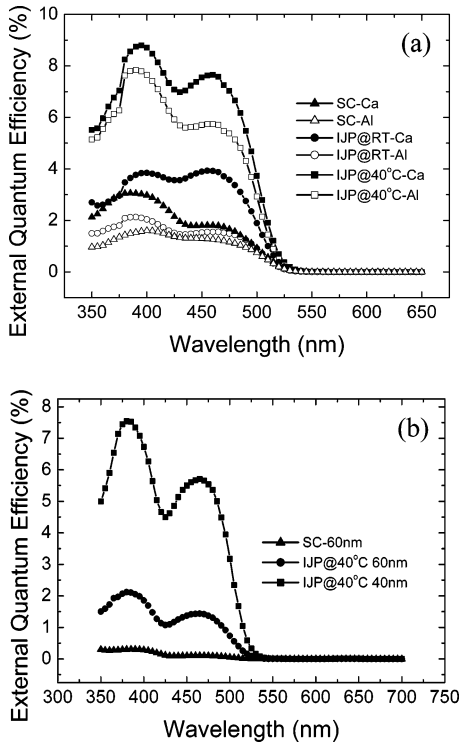

Figure 5. (a) EQE of photovoltaic devices of PFB:F8BT blend (60 nm) prepared by spin-coating (triangles), IJP at room temperature (circles), and IJP at 40 °C (squares), using PEDOT:PSS as anode, and Al (empty symbols) or Ca (filled symbols) as cathode; (b) EQE of photovoltaic devices of TFB:F8BT blend prepared by spin-coating (60 nm, triangles) and IJP at 40 °C (circles for 60 nm film, squares for 40 nm film), using PEDOT:PSS and Ca as electrodes.

Table 1. Photoluminescence (PL) Efficiency (in %) of Films Produced by Different Processes under Laser Excitation of 457 nm

material[a]	spin-coating	inkjet printing at RT	inkjet printing at 40 °C
F8BT	77	76	
PFB:F8BT blend	32	30	27
TFB:F8BT blend	55	45	37

[a] Both PFB:F8BT and TFB:F8BT blends are 50:50 in composition.

better charge transport/collection despite the increased energy barrier for electrons to reach cathode when Al cathode is changed to Ca.

Efficient photovoltaic devices can also be fabricated by printing the TFB:F8BT blend, despite a very poor photovoltaic efficiency from this blend when it is prepared by spin-coating. Results are compared in Figure 5b. For a film of about 60 nm thickness, the EQE of IJP blend device reaches a maximum of about 2% at the wavelength of ~380 nm, using Ca as the cathode. Higher efficiencies can be produced when film thickness is reduced to 40 nm despite less absorption. Devices prepared from spin-coated blends of this thickness suffer from high leakage currents, which may arise from too thin TFB-rich domains and excessive pinholes. The spin-coating process tends to accentuate any deformations on the underlying substrate, whereas the dynamic nature of the film forming process during printing seems to help to minimize the influence of defects. The PL efficiencies measured from these TFB blends show that there is a significant quenching when the film is prepared by IJP (Table 1). This suggests that IJP TFB blend does suppress, to a certain extent, the molecular scale phase separation, and this leads to more charge dissociation. Of course, as in the case of PFB:F8BT blend, the reduced size of mesoscale domains also significantly increases the interfacial areas between the two phases, which leads to better charge transport from the bulk of the film to electrodes. Overall, the PV quantum efficiency increase of TFB blend is most probably due to a combination of these two favorable factors.

IV. Conclusion

To summarize, IJP is used to promote finer phase separation in binary polymer blend systems of polyfluorene derivatives. The finer phase separation is attributed to the intrinsically quick drying of small-volume printed droplets. The "coffee-stain" effect causes undesired thickness fluctuations, however, devices are still able to operate well. IJP LEDs of TFB:F8BT blend show good performances and higher efficiency than spin-coated devices at high voltages. IJP photovoltaic devices of both TFB and PFB blends show a much higher efficiency than those from spin-coating. This arises primarily from the finer phase separation promoted by inkjet printing.

Acknowledgment. We thank Dr. C. J. Newsome for valuable discussions. We thank the Engineering and Physical Sciences Research Council and Seiko-Epson for financial support.

References and Notes

(1) Burroughes, J. H.; Bradley, D. D. C.; Brown, A. R.; Marks, R. N.; Mackay, K.; Friend, R. H.; Burn, P. L.; Holmes, A. B. *Nature (London)* **1990**, *347*, 539−541.
(2) Braun, D.; Heeger, A. J. *Appl. Phys. Lett.* **1991**, *58*, 1982−1984.
(3) Greenham, N. C.; Moratti, S. C.; Bradley, D. D. C.; Friend, R. H.; Holmes, A. B. *Nature (London)* **1993**, *365*, 628−630.
(4) Yu, G.; Gao, J.; Hummelen, J. C.; Wudl, F.; Heeger, A. J. *Science* **1995**, *270*, 1789−1791.
(5) Halls, J. J. M.; Walsh, C. A.; Greenham, N. C.; Marseglia, E. A.; Friend, R. H.; Moratti, S. C.; Holmes, A. B. *Nature (London)* **1995**, *376*, 498−500.
(6) Morteani, A. C.; Dhoot, A. S.; Kim, J. S.; Silva, C.; Greenham, N. C.; Friend, R. H.; Murphy, C.; Moons, E.; Ciná, S.; Burroughes, J. H. *Adv. Mater.* **2003**, *15*, 1708−1711.
(7) He, Y.; Gong, S.; Hattori, R.; Kanicki, J. *Appl. Phys. Lett.* **1999**, *74*, 2265−2267.
(8) Halls, J. J. M.; Arias, A. C.; MacKenzie, J. D.; Inbasekaran, M.; Woo, E. P.; Friend, R. H. *Adv. Mater.* **2000**, *12*, 498−502.
(9) Kim, J. S.; Ho, P. K. H.; Murphy, C. E.; Friend, R. H. *Macromolecules* **2004**, *37*, 2861−2871.
(10) Corcoran, N.; Arias, A. C.; Kim, J. S.; MacKenzie, J. D.; Friend, R. H. *Appl. Phys. Lett.* **2003**, *82*, 299−301.
(11) Snaith, H. J.; Friend, R. H. *Thin Solid Films* **2003**.
(12) Arias, A. C.; MacKenzie, J. D.; Stevenson, R.; Halls, J. J. M.; Inbasekaran, M.; Woo, E. P.; Richards, D.; Friend, R. H. *Macromolecules* **2001**, *34*, 6005.
(13) Morteani, A. C.; Sreearunothai, P.; Herz, L. M.; Friend, R. H.; Silva, C. *Phys. Rev. Lett.* **2004**, *92*, art. no.-247402.
(14) Sirringhaus, H.; Kawase, T.; Friend, R. H.; Shimoda, T.; Inbasekaran, M.; Wu, W.; Woo, E. P. *Science* **2000**, *290*, 2123−2136.
(15) de Gans, B. J.; Duineveld, P. C.; Schubert, U. S. *Adv. Mater.* **2004**, *16*, 203−213.
(16) deMello, J. C.; Wittmann, H. F.; Friend, R. H. *Adv. Mater.* **1997**, *9*, 230−232.
(17) Kawase, T.; Sirringhaus, H.; Friend, R. H.; Shimoda, T. *Adv. Mater.* **2001**, *13*, 1601−1605.
(18) Deegan, R. D.; Bakajin, O.; Dupont, T. F.; Huber, G.; Nagel, S. R.; Witten, T. A. *Nature (London)* **1997**, *389*, 827−829.

(19) Deegan, R. D.; Bakajin, O.; Dupont, T. F.; Huber, G.; Nagel, S. R.; Witten, T. A. *Phys. Rev. E* **2000**, *62*, 756−765.
(20) Lide, D. R., Ed. *Handbook of Chemistry and Physics*; CRC: Boca Raton, FL, 1991.
(21) Lampert, M. A., Mark, P., Eds.; *Current Injection in Solids*; Academic Press: New York, 1970.

MA0503413